

# Strain Sensor from Tapered Fibres

Celaschi Sergio<sup>1\*</sup>, Guerra Christiano P.<sup>1</sup>, Biazoli Claudécir<sup>1</sup>, Cordeiro Cristiano B.<sup>2</sup>, and Grégoire Nicolas<sup>3</sup>

<sup>1</sup>CTI Renato Archer, Campinas 13069-901, Brazil

<sup>2</sup> Dept. Eletrônica Quântica - IFGW, UNICAMP, Campinas 13083-859, Brazil

<sup>3</sup>Centre d'Optique, Photonique et Laser, Université Laval, Québec, Canada, G1V 0A6

**Abstract.** A new all fibre, and low transmission loss, digital optical strain sensor is proposed. This sensor behaves as a Coaxial Mach-Zehnder interferometer. Special depressed cladding single-mode fibre DCF was tapered down to the micrometer scale presenting FSR in the nm range. The sensor is modelled to probe up to  $\pm 0.2\%$  strain when under expansive or compression stresses, returning 20 optical Power Transfer Turning Points (PTTP) at 1575 nm transmitted wavelength.

## 1 Introduction

Devices fabricated by tapering optical fibres, enable additional effects and applications other than those reported using bulky optical fibres [1]. Analogue fibre optics sensing devices based on interferometer's principles are crucial for many applications. Unfortunately, these sensors have as disadvantage a low linear dynamic range. On the other hand, the ease of fabrication of tapered fibre-based devices contributes to their use in applications such as: Brillouin optical sensors [2], tuneable acoustic-optical filters, super continuous radiation generation, among others applications [3], useful in Internet of Things (IoT). For these reasons, the concept of multimodal interference has been studied aiming at the development of different devices. Devices intrinsically manufactured from tapering single-mode fibres (SMF) allow the generation and propagation of selected super-modes, causing interference at the output of the multimode (MM) tapered section. As a result, low loss transmitted optical power may be observed at specific wavelengths. In addition, when this SMF has a Depressed Refractive Index profile (DCF), and the adiabatic condition holds at the tapered section, this structure behaves as a Coaxial Mach-Zehnder interferometer (CMZI) [3]. The interrogation of such sensor occur acting externally on either the MM optical path, or on the super-modes speed (external refractive index).

In this work, an all-fibre digital strain sensor based on a taper from a DCF is proposed. Our fabricated tapered-based CMZI senses external force fields acting on the optical path of the excited super-modes.

### 1.1 Materials, principles and methods

The DCF has been specified, and manufactured to enable HE<sub>11</sub> HE<sub>12</sub> mode coupling at the adiabatic tapering section [4]. The core and cladding radius and refractive index parameters of the DCF is shown in Figure 1. Determining which profile results from stretching a fibre into a given heat source with its own temperature distribution is a complex fluid mechanics problem.

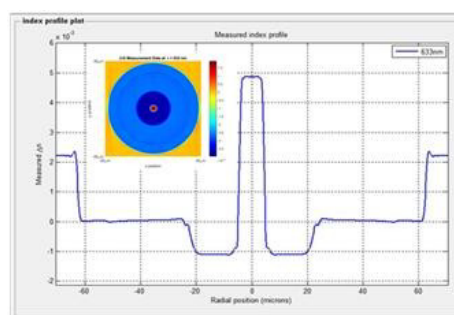


Fig.1. Refractive index profile of the DCF. Inset 2-D measurement data at 633 nm.

This problem was previously modelled by a coupled of partial differential equations and solved numerically [2]. However, no knowledge of fluid mechanics other than mass conservation is required to describe a simple model in which a fixed length of fibre is heated to a constant/uniform temperature and stretched. In this approach [4], simple mathematical equations (Eq. 1 and 2) are obtained for the shape of the profile,

$$\rho(\alpha, L_o, z) = \rho_0 \left[ 1 + \frac{2\alpha(z_f - z)}{(1-\alpha)L_o} \right]^{-1/2\alpha} \quad (1)$$

$$L_w = L_o + 2 \cdot \alpha \cdot Z_f \quad (2)$$

Where  $\phi(\alpha, L_o, z) = 2\rho(\alpha, L_o, z)$  is the diameter of the fibre in the profile region.  $\rho_o$  is the radius of the fiber outside the tapered region,  $\alpha$  is the linear rate of change in the length of the heated zone with the fiber extension.  $L_o$  is the initial length of the heated zone,  $Z_f = Z + L_w/2$  the final extension of that region on the axial axis  $z$  of the fibre, and  $L_w$  the length of the waist region.

## 2 Experimental data and discussion

Three fibre tapers with different parameters, as shown in Table 1 were modelled and manufactured. A micro-torch, displaced in the longitudinal direction was used. The DCF was pulled using step motors.

\* Corresponding author: [sergio.celaschi@cti.gov.br](mailto:sergio.celaschi@cti.gov.br)

**Table 1.** Tapers parameters, model and experiments

| Sample | $\alpha$ | $L_o$ (mm) | $D_w$ ( $\mu\text{m}$ ) | $L_w$ (mm) | $Z$ (mm) | $L_{total}$ (mm) |
|--------|----------|------------|-------------------------|------------|----------|------------------|
| 1      | -0.1     | 14         | 3.9                     | 6.7        | 38.5     | 84               |
| 2      | -0.1     | 14         | 10.6                    | 8.5        | 30       | 68.5             |
| 3      | -0.1     | 14         | 27.8                    | 10.4       | 20       | 50.4             |

The resulting taper profiles, and fitting curves, according to Eqn. (1) and (2), are presented in Fig.2.

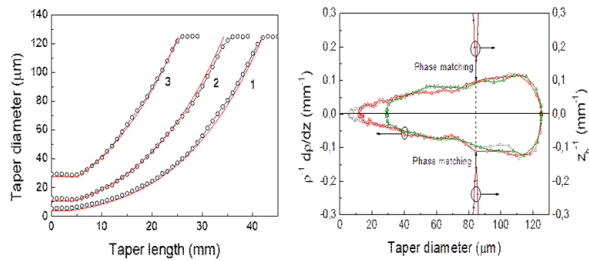


Fig.2. Left: Half taper profiles for three different heat-and-pull processes. Open circles are measured data. The solid lines are fittings to the analytic model, using parameters from Table 1. Right: Adiabatic condition  $(1/\rho)d\rho/dz < 1/z_b$  where  $z_b$  is the beat length between  $HE_{11}$  and  $HE_{12}$ .

During the heat-and-pull process a number of oscillations (inset of Figure 3) is observed in the transmitted optical power, and defined as Power Transfer Number (PTN). PTN presents an exponential dependence for different taper elongations. According to mode coupling theory, under adiabatic condition [6],  $PTN(\alpha, L_o, Z_f) = (2/\pi) \int_0^{Z_f} \Delta\beta(\alpha, L_o, z) \cdot dz$  where  $\Delta\beta$  is the difference for  $HE_{11}$  and  $HE_{12}$  propagation constants.

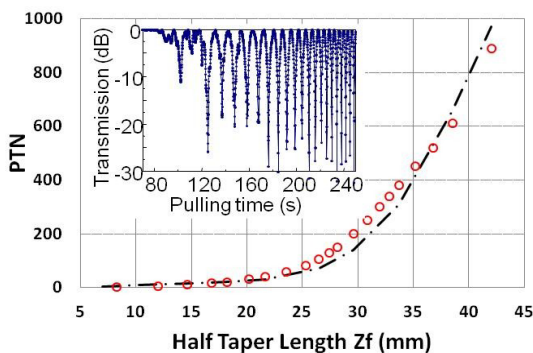


Fig.3. Power transfer number PTN versus  $1/2$  taper length for different taper elongations. Broken line, mode coupling theory fitting. Inset - transmitted power at 1575 nm as a function of the first 240 seconds of the heat-and-pull process.

The intrinsic sine square response in transmitted power (@ 1575 nm) to external mechanical loads of sample #1 can be seen in the inset of Figure 4. The output power experiences a number of Power Transfer Turning Points (PTTP) when under stress, and this PTTP is directly

proportional to  $\Delta L/L_o$  (Figure 4). An intrinsic sine square transfer function has two PTTP per cycle. Submitted to 0.02 Newton it elongates by  $\Delta Z = 180 \mu\text{m}$ , which is equivalent to an increase  $\Delta PTN = 10$ , and a number of  $PTTP = 2 \cdot \Delta PTN = 20$ . It can be clearly noticed from Figure 4 that the digital sensor operates counting the PTTP when under traction or compression along its longitudinal direction. Negligible hysteresis was observed between traction and compression. Transmission and detection of two distinct wavelengths spectrally spaced by an odd multiple of a quarter of the FSR are necessary for sensing compression and traction. Finally, the proposed sensor can be a potential candidate for monitoring strains. In special, in environments under high electromagnetic interference or under risk of explosion where conventional electric strain sensors might fail. Moreover, several of these sensors can be distributed along one fiber making it possible to cover large areas.

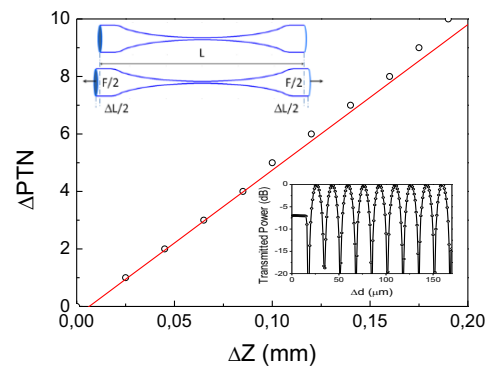


Fig.4. Experimental  $\Delta PTN$  as a function  $\Delta Z$  (open circles). Red line represents the analytic model for the digital response of the sensor for the strain range  $\Delta L/L_o$ . Inset shows 20 PTTP of the transmitted power as a function of taper elongation. A negligible hysteresis value of  $-0.4 \mu\text{m}$  was observed.

**S. Celaschi acknowledges FINEP/MCTIC financial support (01.16.0053.01) under project Plat IoT, granted by FUNTTEL. CNPq sponsors authors C.P. Guerra, and C. Biazoli under PCI scholarships (300473/2018-4). This paper reflects only the author's views.**

## References

1. S. Celaschi, G. N. Malheiros-Silveira, *J Lightwave Tech.* **35** (24), pp. 5381, (2017)
2. J. Beugnot, S. Lebrun, G. Pauliat, et al. *Nature Commun.* **5**, 5242 (2014)
3. G. Brambilla et al., *Advances in Optics and Photonics* **1**, 107–161 (2009)
4. S. Celaschi, G. N. Silveira, et al., in *OSA Latin Am. Optics and Photonics Conf*, Lima, p. W3B.7, (2018)
5. T.A. Briks, Y.W. Li, " *J Lightwave Tech.* **10** (4), 432, (1992)
6. A. W. Snyder and J. D. Love, *Optical Waveguide Theory*, Boston, MA: Springer US, (1984).